Product Selectivity Control and Organic Oxygenate Pathways from Partial Oxidation of Methane in a Silent Electric Discharge Reactor

David W. Larkin, Liming Zhou, Lance L. Lobban, and Richard G. Mallinson*

Institute for Gas Utilization Technologies and School of Chemical Engineering and Materials Science, University of Oklahoma, 100 E. Boyd, Room T 335, Norman, Oklahoma 73019

This study of methane conversion involves the use of a glass dielectric interposed between metal electrodes and applies kilovolt AC voltage and 118-W power with frequencies in the range of 173−264 Hz. The geometry of the system is cylindrical, with gas flowing axially in the annulus between two electrodes. The partial oxidation reactions in this configuration produce methanol, formaldehyde, formic acid, methyl formate, ethane, hydrogen, water, carbon monoxide, and carbon dioxide. The outer electrode is maintained at a low temperature (12 or 15 °C), allowing the organic oxygenates to condense on the plate itself inside the reactor. The results show, through residence-time experiments, that methane and oxygen react to form methanol, which further reacts to form formaldehyde, methyl formate, and formic acid. Increasing the gas gap from 4.0 to 12.0 mm decreases the reduced electric field from 30 to 18 V/(cm Torr), which results in a shift in the product distribution from organic oxygenate products to ethane, ethylene, and acetylene. This is because the energy deposition directed toward oxygen dissociation decreases and the energy deposition directed toward methane and oxygen excitations increases. Finally, this work shows that increasing the pressure from 1 to 2 atm with a 1.9-mm gas gap decreases the energy consumption of the system per molecule of methane converted by 35% because the feed concentration doubles, while maintaining 46% selectivity in organic oxygenate products because the reduced electric field strength has a significant fraction of the energy directed toward oxygen dissociation under these conditions.

Introduction

Natural gas is looked upon as a desirable fuel because it is clean-burning and has vast reserves worldwide. Many of the these reserves, however, are located in remote areas, so that it is economically infeasible to transport the gas via pipeline. One alternative is to convert the natural gas into an organic liquid, such as methanol, at the production site, which would greatly reduce the transportation costs. The current commercial methanol synthesis technology is an energy-intensive two-step process that might not be economical when the natural gas is in remote places or is expensive to obtain.

A desirable alternative is the direct partial oxidation of methane to methanol as a one-step process could potentially reduce both capital and operating costs. Currently, no economical one-step direct partial oxidation of methane to methanol process is known; however, plasma reactors might be a possible solution. Already, these reactors are being commercially used to produce ozone. In addition, research has been done with these reactors on NO_x, SO_x, toxic gases, volatile organic compounds, and hazardous emissions control.[1] These reactors can generate equilibrium or nonequilibrium plasmas. Equilibrium plasmas are plasmas in which the electrons and neutral species have the same kinetic energies, whereas in nonequilibrium plasmas, the kinetic energies of the electrons are much higher than those of the neutral species. The latter type of plasma can be created through the use of a dielectric barrier discharge (DBD) reactor.[2,3]

Several studies on the direct partial oxidation of methane to methanol using a DBD reactor have been done. Bhatnagar and Mallinson showed that decreasing the methane/oxygen ratio increases the methane conversion rate.[4] In addition, Larkin et al. demonstrated that increasing the partial pressure of CO_2 for a methane/oxygen/carbon dioxide feed further inhibits CO_2 production.[5] Also, Zhou et al. proposed important chemical pathways occurring in a methane/oxygen system within a DBD reactor.[6]

The electron energy distribution in a DBD reactor can be altered by changing various system parameters (e.g., gas gap and system pressure). This in turn affects the energy deposition directed toward the various electron/gas species collision processes. Hence, the chemistry occurring within the reaction zone can be influenced by changing the electrical properties of a gas-phase system within the DBD reactor.

These electrical properties can be characterized through Bolsig, an electron Boltzmann equation solver by Kinema Software and CPAT.[7] This electron Boltzmann solver is designed for systems that have uniform steady-state electric fields (E) with weakly ionized gases, which is the case for a DBD system.[7] This program numerically solves for the Boltzmann equation, shown below, that describes the electron energy distribution function (f) in terms of space (x), velocity (v), and time (t).[2,7,8]

$$\frac{\partial}{\partial t}f(x,v,t) + a\nabla_v f(x,v,t) + v\nabla_x f(x,v,t) = J[f(x,v,t)] \quad (1)$$

According to the presentation of Eliasson and Kogelschatz[2] regarding the Boltzmann equation, a is the acceleration term, $a = (cE)/m$ (c = electron charge, m = mass of electron), which is proportional to the force from the electric field (E) acting upon the electron. The term on the right-hand side of the equation, $J[f(x,v,t)]$, is the collision term. It accounts for the electron energy

10.1021/ie010298h CCC: $20.00
Published on Web 10/13/2001

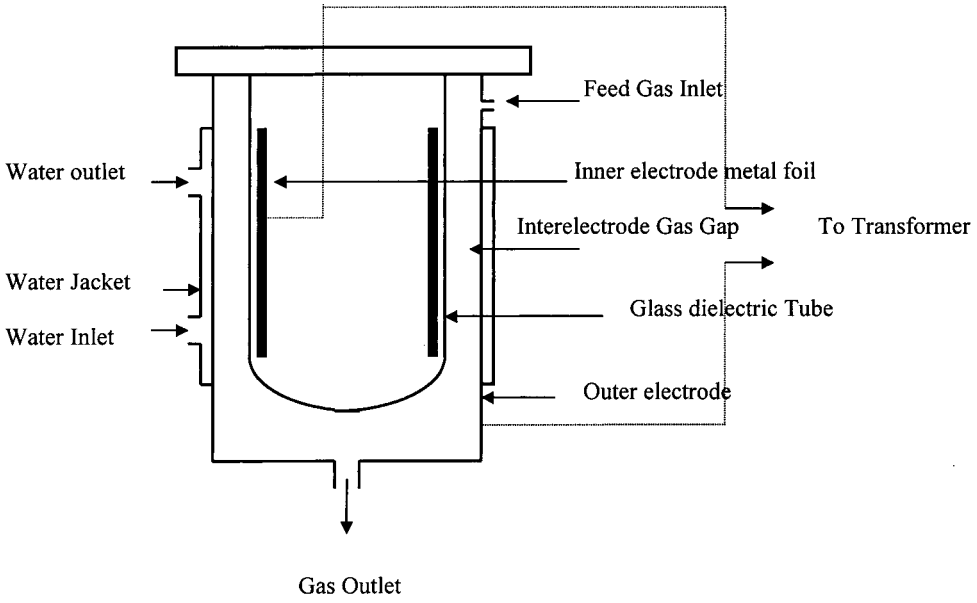

Figure 1. Annular reactor.

distribution change due to collisions between electrons and gas species present in the reaction zone.[2] Therefore, this program can determine the energy deposition directed toward the various collision processes: elastic, inelastic, ionization, and attachment. Because the DBD system has a uniform steady-state electric field at high pressure (1 atm or greater), the electron energy distribution becomes simply a function of velocity. Once $f(v)$ is known, the average electron energy (e_{avg}) can be found for a given reduced electric field using[9]

$$e_{avg} = \int_0^\infty e(v)\, f(v)\, dv \qquad (2)$$

where

$$e(v) = \frac{1}{2} m v^2$$

In addition, because the electron energies within the system are affected by the electric field strength and interactions with the gas species present, the average electron energy can be described as a function of the reduced electric field (E/P), which is the electric field divided by the system pressure (P), at the conditions of breakdown. Changes that increase the reduced electric field result in an increase in the average electron energy. The reduced electric field is also related to the breakdown strength and is a function of the breakdown voltage (V), gas gap distance (D), and system pressure ($E = V/D$ and therefore $E/P = V/DP$). Increasing the system pressure or gas gap distance will result in a decrease in the reduced electric field and, hence, the average electron energy within the system.[2]

This work, which is a continuation of previous efforts,[4,5,10,11] uses a DBD reactor to directly partially oxidize methane to organic oxygenates, such as methanol. To determine the effects of the reduced electric field and, therefore, the average electron energy on product selectivities, methane and oxygen conversions, and energy consumption within the system, the gas gap distance was varied. In addition, the effects of changing the system pressure from 1 to 2 atm was studied to determine the similarities with the results of the gap-distance experiments at similar reduced electric field strengths. Further, the effect of pressure at different gap distances in regards to organic oxygenate production is also investigated.

Previous results have shown that a 3:1 methane/oxygen feed has a greater methane conversion rate than a pure-methane feed (with all other experimental parameters held constant).[5] In addition, organic oxygenate products were formed only when oxygen was present in the feed. This work examines the effect of partial pressure of oxygen on the methane reaction rate, energy efficiency, and product selectivity for methane/oxygen systems at 1 and 2 atm. This is done at both these system pressures by decreasing the methane/oxygen ratio from 5:1 to 2:1.

Finally, this study conducts residence-time experiments in a DBD reactor. These experiments are conducted in order to better understand the sequential and parallel product-formation pathways that occur within the methane/oxygen system.

Experimental Section

Methane and oxygen are fed to the DBD reactor, shown in Figure 1, by mass flow controllers (Porter Instrument Company). The methane/oxygen feed enters through the top of the reactor and flows axially downward in a gas gap between two concentric cylinders. The inner cylinder is made of glass and acts as the dielectric. This glass dielectric cylinder has a stainless steel metal foil on its inner wall that acts as an electrode. The metal foil length is 30.5 cm in all experiments except for the residence-time experiments in which it is 17.8 cm. The outer cylinder is also made of stainless steel, and its inner wall, with a length of 43.2 cm, acts as the other electrode. Thus, the DBD reactor has a capacitive nature with a glass dielectric that evenly distributes the "microdischarges" and limits their duration.[12] The reactor is cooled by a water jacket that surrounds the outer reactor shell.

The product stream exits from the bottom of the reactor and flows to a liquid trap cooled by dry ice and acetone (−55 °C). Organic oxygenates (principally methanol, formaldehyde, methyl formate, and formic acid) and water are collected in the trap. Some of these products

Table 1. Experimental Reproducibility[a]

expt	mol of CH_4 converted (mol/min)	eV/molecule of CH_4 converted	H_2 selectivity	mol % CH_4 converted	mol % O_2 converted	% C selectivity[b] (molar basis)							
						CO_2	CO	ethane	M	MF	FA	F	sum
1	0.0009	79	18	10	61	13	16	5	19	5	17	10	85
2	0.0010	76	16	10	56	13	16	5	18	6	16	13	87

[a] CH_4/O_2 feed ratio = 5:1, gap distance = 1.9 mm, power = 118 W, pressure = 1 atm, residence time = 29 s, water temperature in water jacket = 15 °C. [b] M = methanol, MF = methyl formate, FA = formic acid, F = formaldehyde, sum = sum of carbon product selectivities (molar basis).

can potentially condense within the reactor because of the low system temperature and are then carried out by the gas stream. The remaining effluent gas stream exits the liquid trap and flows to a Carle 400 AGC instrument with a hydrogen analysis system. The liquid product collected from the liquid trap is analyzed on a Varian 3300 GC with a Porapak Q column.

The DBD reactor receives its AC power from an Elgar model 501 SL power supply. The voltage range for the Elgar is from 0 to 130 V, its current range is from 0 to 5.8 A, and its frequency range is from 45 to 5000 Hz. It has a maximum power output of 500 W. A CBK precision generator allows the Elgar power system to produce a sinusoidal waveform at a desired frequency. A 15060 P Franceformer transformer steps up the voltage and applies it to the DBD reactor. The breakdown voltage for the annular reactor is measured using a Tektronix P6015A high-voltage probe in conjunction with a Tektronix TDS 754C digital oscilloscope.

The power is measured with a Microvip 1.2 Energy Analyzer on the primary side (primary side = low voltage side of transformer). This allows the system's energy consumption to be determined per molecule of methane converted (The energy consumption as used in this work is in electronvolts per molecule of methane converted and 1 eV/molecule of CH_4 converted = 96.4 kJ/mol = 1.67×10^{-3} kWh/g). As a result of measuring the power on the primary side, the energy losses from the DBD reactor, high-voltage wires, and transformer are all included in the measured value. Additionally, the components (DBD reactor, high-voltage wires, and transformer) have not been optimized to minimize these energy losses, and therefore, this work underestimates how energy efficient this process could be.

To demonstrate that the experiments performed in this work can be acceptably reproduced, Table 1 compares two 5:1 methane/oxygen experiments at identical conditions. The material balances (carbon molar basis) for all of the experiments in this work are close to closing (80−100%). Potentially, the unaccounted carbon comes from undetected products in the gas phase as no solid residue was found within the reactor after experiments.

In all experiments, the power input was 118 W, which was sufficient to convert a significant amount of the methane. The frequency in each experiment was set such that the power factor on the low voltage side of the transformer was 1

$$\text{power factor} = \cos(\theta) = \frac{\text{power}_{\text{avg}}}{\text{voltage}_{\text{RMS}} \times \text{current}_{\text{RMS}}}$$

The water temperature within the water jacket for this work was set at 12 or 15 °C. (Only the residence-time experimental series had a 12 °C water temperature.) Both of these temperatures allowed for the in situ removal of organic oxygenates from the reaction zone, as seen in previous work,[10] for experiments with residence times of 5 s or greater.

The first series of experiments varied the gas gap distance from 1.9 to 12.0 mm to determine how changes in the reduced electric field strength affected the results of a 2:1 methane/oxygen system. The gas gap was increased by using smaller-diameter glass dielectric tubes. When the gas gap was increased from 1.9 to 12.0 mm, the gas feed flow rate was also increased to maintain a constant residence time of 1 min. Further, when the gap distance was changed from 1.9 to 12.0 mm, the frequency was increased from 174 to 216 Hz to maintain the power factor at a value of 1, as the capacitance of the system changes when the gas gap is altered. In all gap-distance experiments, the reaction area was 688 cm^2.

The second series of experiments varied the system pressure from 1 to 2 atm for a 2:1 methane/oxygen system with a residence time of 29 s so that the methane and oxygen conversions would be similar to those of the gap-distance experiments. This provides a comparison of product selectivities between the pressure and gap-distance experimental series at similar reduced electric fields. The pressure experimental series had a gap distance of 4.0 mm and a reaction electrode area of 688 cm^2. At 1 atm, the frequency was set at 173 Hz, and at 2 atm, it was 241 Hz.

For the third series of experiments, the methane/oxygen feed ratio was varied from 5:1 to 2:1 at 1 and 2 atm with a gap distance of 4.0 mm, an electrode reaction area of 688 cm^2, and a residence time of 29 s. The frequency was 173 Hz at 1 atm and 241 Hz at 2 atm.

The fourth series of experiments varied system pressure from 1 to 3 atm while maintaining the gap distance at 1.9 mm and the methane/oxygen feed ratio at 5:1. This was done to determine the effects of pressure on a system in which a significant amount of the energy input into the system was directed toward oxygen dissociation at all system pressures as a result of the smaller gap distance (1.9 as opposed to 4.0 mm). The electrode reaction area for these experiments was 688 cm^2, and the residence time was 29 s. The frequency was adjusted to maintain the power factor at 1, so that, at 1 atm, it was 167 Hz; at 2 atm; it was 217 Hz, and at 3 atm, it was 264 Hz.

The last series of experiments varied the residence time from 2.5 to 40 s to better determine the carbon pathways occurring within the system. The reaction area for these experiments was 430 cm^2, and the frequency was 198 Hz.

Finally, Bolsig, the numerical electron Boltzmann solver by Kinema Software and CPAT, was used to plot all of the energy deposition graphs (energy deposition directed toward a given collision process as a function of reduced electric field strength). In addition, it was used to determine the average electron energy within methane/oxygen system for a given reduced electric field strength.[7,13]

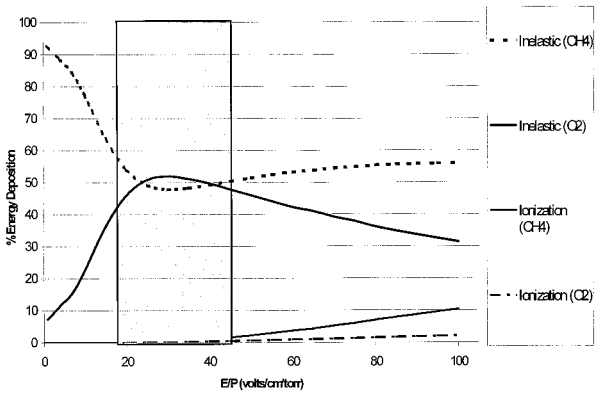

Figure 2. Energy deposition (group processes) vs *E*/*P* (2:1 CH_4/O_2 system).

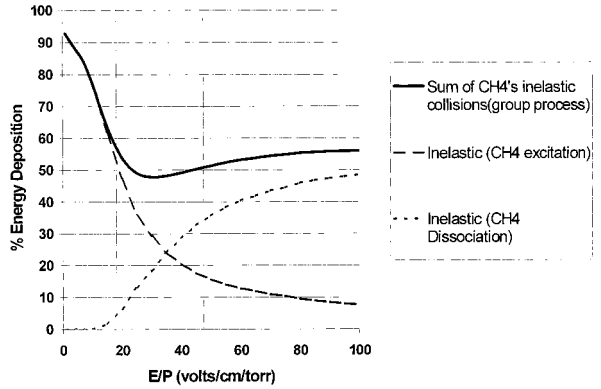

Figure 3. Energy deposition vs *E*/*P* (2:1 CH_4/O_2 system).

Table 2. Electrical Parameters[a]

gap distance (mm)	1.9	4.0	6.7	12.0
E/*P* [V/(cm Torr)]	49.0	30.0	24.0	18.0
average electron energy (eV)	5.0	4.2	4.0	3.6

[a] 2:1 CH_4/O_2 system at 1 atm.

Results and Discussion

As previously mentioned, altering the gas gap affects the reduced electric field of a DBD system. Table 2 shows how the electrical and discharge properties change when the gas gap is varied from 1.9 to 12.0 mm. Increasing the gas gap distance decreases the reduced electric field strength (*E*/*P*), and this results in a decrease in the average electron energy of the plasma. Decreasing the reaction zone's average electron energy in turn affects the energy deposition directed toward the various types of collision processes. Figure 2 shows the energy deposition for the significant collision processes as a function of reduced electric field strength (*E*/*P*) in a barrier discharge reactor for a 2:1 methane/oxygen system. The experimental operating region for this study lies within the gray region seen in this figure. Within this operating region, at least 97% of the energy being put into the reaction zone is directed toward inelastic methane and oxygen collision processes. Processes such as attachment ($e^- + A_2 \rightarrow A_2^-$), ionization ($e^- + A_2 \rightarrow A_2^+ + 2e^-$), and elastic ($e^- + A_2 \rightarrow e^- + A_2$) collision processes are not significant in this range.

Figure 3 separates the energy deposition for the inelastic methane collision processes into its two primary components: methane excitation and methane dissociation. The two components have electron-impact formation energy ranges of 0.2−0.4 eV and 9.0−12.0 eV, respectively. The figure shows that, within the experimental operating region, when the reduced electric field is decreased, the energy deposition directed toward methane excitation increases, whereas that directed toward methane dissociation decreases. When the reduced electric field is decreased, the average electron energies decrease, and the fraction of electrons capable of dissociating methane is reduced. This also means that the fraction of electrons capable of exciting, but not dissociating, methane molecules increases and that the energy fraction deposited into the excitation process increases.

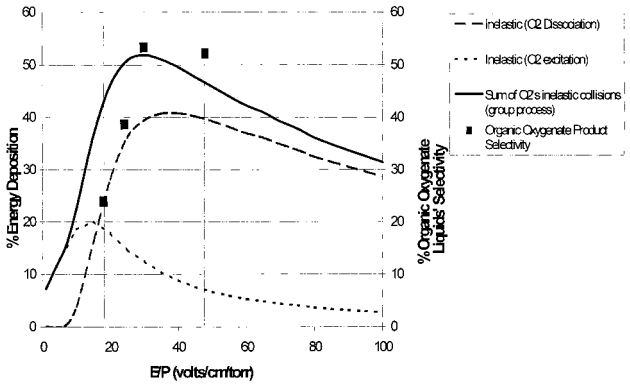

Figure 4. Energy deposition and organic oxygenate product selectivity vs *E*/*P* (2:1 CH_4/O_2 system, 118-W power input, 15 °C water jacket temperature).

Figure 4 separates the energy deposition for the inelastic oxygen collision processes into its two components: oxygen excitation and oxygen dissociation. The two components have electron impact formation energy ranges of 0.2−4.0 eV and 6.0−8.4 eV, respectively. Within the experimental operating region seen in this figure, a decrease in the reduced electric field strength results in an increase in the energy deposition directed toward the excitation of the oxygen molecules without dissociation. In this same range, the energy deposition directed toward oxygen dissociation remains around 40% for reduced electric field values above 30 V/(cm Torr) and decreases significantly below this value. This decrease occurs because the average electron energy decreases to the point that there is a significant reduction in the fraction of electrons having enough energy to dissociate oxygen molecules and an increasing portion of the electrons that have only enough energy to excite oxygen (and methane) molecules.

In addition to the inelastic oxygen collision processes, Figure 4 also shows the organic oxygenate product selectivity (organic oxygenate product selectivity = sum of organic oxygenate selectivities) as a function of reduced electric field. The results show that, for a change from 48 to 30 V/(cm Torr), the organic oxygenate selectivity and the energy deposition going into oxygen dissociation stay relatively constant. However, from 30 to 18 V/(cm Torr), the organic oxygenate product selectivity and the energy deposition going into oxygen dissociation both sharply decrease. Finally, the energy deposition going into oxygen excitation without dissociation does not follow the organic oxygenate product selectivity trend, as it increases when the reduced electric field decreases from 48 to 18 V/(cm Torr). These results suggest that an atomic oxygen species generated from oxygen dissociation is responsible for the direct partial oxidation of methane to organic oxygenate species.

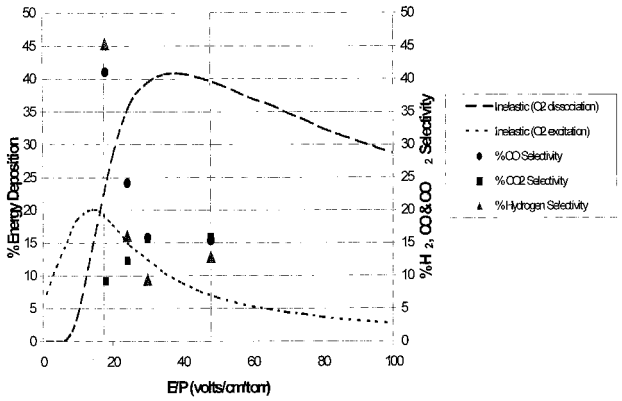

Figure 5. Energy deposition, CO_x selectivity, H2 selectivity vs *E*/*P* (2:1 CH_4/O_2 system, 118-W power input, 15 °C water jacket temperature).

Figure 5 shows the CO and CO_2 selectivities for the gap-distance experiments as functions of reduced electric field. In addition, the H_2 selectivity and energy deposition directed toward the two inelastic oxygen processes are included in this figure. As can be seen in the figure, the CO and CO_2 selectivities and energy deposition directed toward oxygen dissociation remain relatively constant in the range from 48 to 30 V/(cm Torr), but from 30 to 18 V/(cm Torr), the CO selectivity increases while the CO_2 selectivity decreases. Because the energy deposition directed toward oxygen dissociation decreases over this same reduced electric field range, atomic oxygen species are evidently involved in the oxidation of CO to CO_2. However, as will be seen in the discussion of the pressure experiments, a high CO/CO_2 ratio can be obtained under conditions where significant O_2 dissociation does occur, and this appears to be inconsistent with the above explanation. This point will be discussed further in the same section.

Another factor affecting the CO and CO_2 selectivities, shown in previous work, is that increasing the partial pressure of CO in a methane/carbon monoxide/oxygen system shifts the selectivity from CO toward CO_2 via the water−gas shift pathway.[5] In the range where the CO selectivity is higher, the hydrogen selectivity (and partial pressure) also increases, as also shown in Figure 5. In addition, significant in situ removal of water from the reaction zone via condensation occurs under these conditions over the entire range of reduced electric field. This is shown by the fact that 72% of the water exiting the 12-mm-gap reactor was collected in the liquid phase. Both of these factors inhibit the water−gas shift reaction and CO_2 formation from this pathway.

Finally, Figure 5 shows that the energy deposition directed toward the excitation of oxygen molecules without dissociation increases over the entire operating range, which also suggests that excited oxygen molecules are not nearly as effective at oxidizing CO to CO_2 and are not significantly involved in direct oxidation of other species to CO_2.

Figure 6 shows the gap-distance experiments for the C_2 hydrocarbon selectivity (sum of acetylene, ethylene, and ethane selectivities), the energy deposition directed toward the inelastic methane collision processes and its two components, and the two components for the inelastic oxygen collision processes as functions of reduced electric field. Table 3 shows the acetylene/ethylene/ethane ratio at a given reduced electric field for these experiments. The results show that, when the

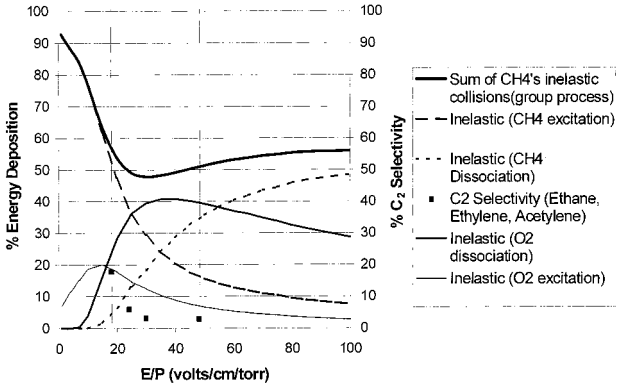

Figure 6. Energy deposition and C_2 selectivity vs *E*/*P* (2:1 CH_4/O_2 system, 118-W power input, 15 °C water jacket temperature).

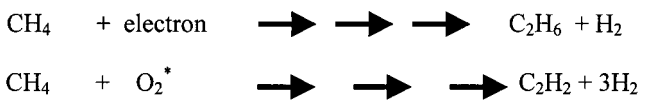

Figure 7. Hydrocarbon formation pathways for C_2 hydrocarbons at low reduced electric fields [*E*/*P* less than 30 V/(cm Torr)].

Table 3. Acetylene/Ethylene/Ethane Ratio for Gap-Distance Experiments

gap distance (mm)	1.9	4.0	6.7	12.0
E/*P* [V/(cm Torr)]	49.0	30.0	24.0	18.0
acetylene/ethylene/ethane	0:0:1	1:0:2	1:0:2	10:1:7
C_2 hydrocarbon sum	3	3	6	18

[a] 2:1 CH_4/O_2 system at 1 atm.

energy deposition directed toward oxygen dissociation decreases and the energy deposition directed toward the inelastic methane collision process increases (the latter as a result of the increase in the energy deposition directed toward methane excitation), the C_2 hydrocarbon selectivity increases. The increased C_2 hydrocarbon selectivity is due to increases in ethane and acetylene production. Caldwell has shown that, in a pure-methane system that, when the gas gap is varied, and therefore the reduced electric field over the same range, the product distribution is composed of ethane and hydrogen with some higher alkanes, but no ethylene or acetylene, and is relatively constant.[15] Those pure-methane results suggest that ethane formation in the 2:1 methane/oxygen system at the lower reduced electric field strengths (where oxygen dissociation is not significant) comes from methane coupling from direct methane activation, as diagrammed in Figure 7. In this range of reduced electric field, oxygen dissociation and its consumption of methane is not significant. Also in this same range, increased oxygen excitation occurs (O_2*), with significant acetylene selectivity. This suggests O_2* involvement in the production of acetylene, as shown in Figure 7. Additional evidence that active molecular oxygen species are involved in C_2 hydrocarbon formation comes from the fact that methane conversion rates for the pure-methane experiments[15] are less than the methane conversion rates in this study. Further, acetylene production becomes negligible at higher reduced electric field strengths, where the energy deposition directed toward oxygen excitation (O_2*) is significantly less than that directed toward oxygen dissociation (O*). In addition, the CO/CO_2 ratio increases over this same reduced electric field range, which suggests that CO formation is favored over CO_2 formation, as already discussed.

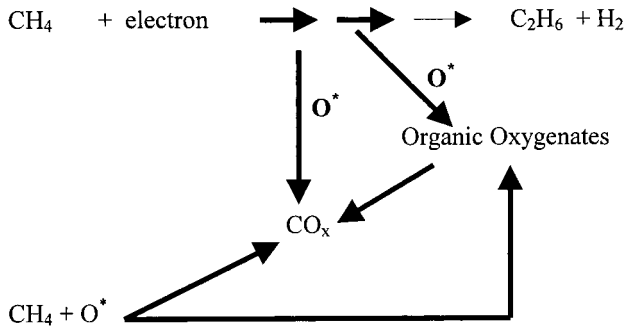

Figure 8. Hydrocarbon formation pathways at high reduced electric fields [*E*/*P* greater than 30 V/(cm Torr)]. Note: This figure includes CH_4 activation that occurs in Figure 7.

At high reduced electric field strengths [$E/P \geq 30$ V/(cm Torr)] the energy deposition directed toward molecular oxygen excitation is small, and therefore, the O_2* hydrocarbon pathway shown in Figure 7 is a minor one with little acetylene formation. The dissociated O* species lead to organic oxygenate formation in part by reacting with activated methane, thus reducing ethane selectivity from the ethane production pathway shown in both Figures 7 and 8. In addition, previous work, as well as residence-time experiments discussed later in this study, provides evidence that a direct oxidative pathway to CO and/or CO_2 exists.[11] Hence, the overall carbon pathway for the 2:1 methane/oxygen system at high reduced electric field strengths includes direct and indirect pathways for CO_x formation, as well as the pathway for organic oxygenate formation, as shown in Figure 8.

For all reduced electric field strengths, little to no ethylene is observed, which suggests that acetylene might be formed, as diagrammed in Figure 7, from the coupling of two CH group species rather than from ethane reacting sequentially to form ethylene and then acetylene, as the thermodynamics of the reaction suggests that this is unlikely to preferentially *not* favor ethylene. Evidence for the presence of CH groups in low-temperature plasmas has been reported by Okumoto et al.,[14] who detected CH groups spectroscopically in a methane/oxygen system using a pulsed DBD reactor. In addition, Caldwell[15] showed that, in a DBD reactor, increasing the partial pressure of hydrogen in an ethane/hydrogen system inhibits the production of ethylene and acetylene. In contrast, these results show that acetylene selectivity increases when hydrogen selectivity increases, which also suggests a different pathway than sequential dehydrogenation.

Figure 9 plots the methane conversion, oxygen conversion, and energy consumption as functions of reduced electric field for the gap-distance experiments. The figure shows that, for a decrease from 48 to 18 V/(cm Torr), the methane and oxygen conversions decrease by 61 and 71%, respectively. The system's energy consumption per molecule of methane converted, however, decreases over the same change in reduced electric field because the methane throughput increases by 82%. The decrease in energy consumption per molecule of methane converted seen for a change from 30 to 18 V/(cm Torr) is largely because of the shift in the energy deposition from oxygen dissociation to methane excitation. In other words, energy is shifting from collision processes that form atomic oxygen, which can react with methane and also carbon monoxide, organic oxygenate products, and hydrogen, to a collision process that forms

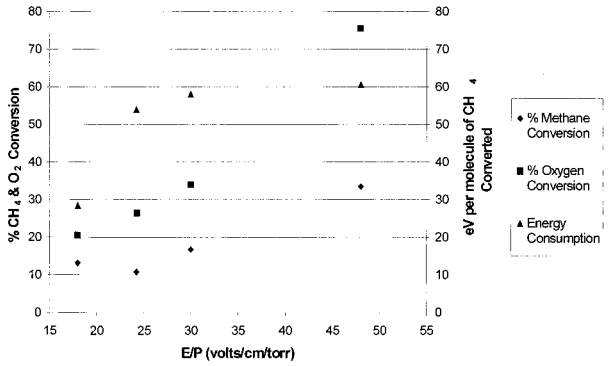

Figure 9. CH_4 conversion, O_2 conversion, and energy consumption (2:1 CH_4/O_2 system, 118-W power input, 15 °C water jacket temperature).

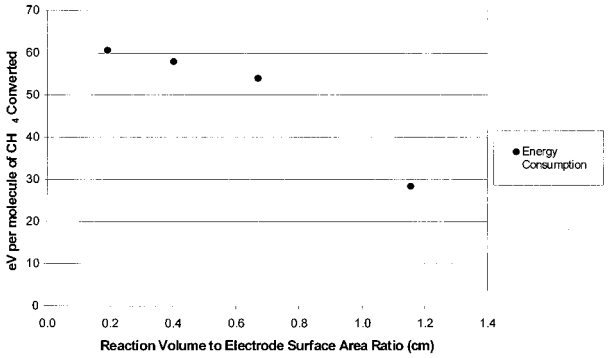

Figure 10. Energy consumption vs reaction volume to electrode surface area ratio (2:1 CH_4/O_2 system, 118-W power input, 15 °C water jacket temperature).

excited methane, which, when it reacts with other species, always consumes methane, thereby increasing the methane reaction rate and, hence, decreasing the energy consumption per molecule of methane converted. In addition, excited oxygen molecules might have a higher probability of *reacting* with methane than other species at the lower reduced electric fields (e.g., CO does not seem to become over oxidized to CO_2 when the energy deposition directed toward oxygen excitation increases).

The system's energy consumption can also be affected by the reaction volume to electrode surface area ratio. Previous work has shown that the ratio of reactor-wall quenching to gas-phase quenching for atomic oxygen is around 1 when the atomic oxygen is within 1 mm of the cylindrical reactor wall (p = 1 bar, bulk gas = helium, reactor temperature = 500 °C). However, when atomic oxygen is within 6 mm of the wall, the ratio of reactor-wall to gas-phase quenching for atomic oxygen significantly decreases.[16] Other research has provided evidence that significant oxygen recombination can take place in a DBD reactor with a 1-mm gas gap.[17] Hence, electrode surfaces can quench radical species, thereby wasting the energy consumed in forming these species because they are no longer able to initiate or propagate reactions. Therefore, increasing the reaction volume to electrode surface area ratio decreases the overall effect of radical quenching at the electrode surface on the overall chemical processes. Figure 10 displays a plot of the system's energy consumption as a function of reaction volume to electrode surface area ratio and shows that the energy consumption does decrease when the ratio is increased from 0.2 to 1.2.

Another way of decreasing the reduced electric field strength is by increasing the pressure within the

Table 4. Pressure Experimental Results[a]

reactor pressure (atm)	*E*/*P* [V/(cm Torr)]	eV/molecule of CH_4 converted	mol of CH_4 converted (mol/min)	% conversion		% selectivity[b]					
				CH_4	O_2	H_2	CO	CO_2	C_2[c]	organic oxygenate liquids	sum[d]
1	30	48	0.0015	8	22	8	16	13	1	59	89
2	23	26	0.0028	9	17	39	33	8	17	37	95

[a] 4.0-mm gap distance, 2:1 CH_4/O_2 feed ratio, 1-min residence time, 118-W power input. [b] Selectivity for carbon compounds is on a carbon molar basis. [c] C_2 represents ethane, ethylene, and acetylene. [d] Sum = sum of carbon selectivities (molar basis).

system. In this series of experiments, the system pressure was increased from 1 to 2 atm in a 2:1 methane/oxygen system with a 4.0-mm gap distance. This was done to support the conclusion that changes in the reduced electric field and the resultant changes in the electron energy are a key variable that controls selectivity between organic oxygenates and C_2 species and between CO and CO_2. The results of the 4.0-mm-gap 2:1 methane/oxygen experiments, presented in Table 4, show that, for a increase from 1 to 2 atm, the organic oxygenate sum decreases from 59 to 37%, and the C_2 selectivity increases from 1 to 17%. The change in the reduced electric field from 30 to 23 V/(cm Torr) is in the region where the energy deposition directed toward oxygen dissociation decreases and that directed toward methane and oxygen excitations increases, as shown in Figures 3 and 4. This is consistent with the behavior in the gap-distance experiments. In addition, doubling the system pressure causes the methane feed concentration to double, which also promotes methane coupling reactions. As for CO and CO_2, for an increase from 1 to 2 atm, the CO/CO_2 ratio increases from 1.2:1 to 4.1:1. This is also consistent with the observations from the gap-distance results. At 2 atm, 81% of the water exiting the reactor is in the liquid phase. Thus, water in the gas phase, which can participate in the water−gas shift reaction, does not appear to participate in a major reaction pathway. Finally, increasing the system pressure from 1 to 2 atm decreases the energy consumption per molecule of methane converted by 46%. Assuming positive-order kinetics, the methane reaction rate can be expected to increase because of the doubling of the feed partial pressure. In addition, the energy consumption per molecule of methane converted also decreases because some of the energy input into the system is shifted from processes that do not directly consume methane to processes that do. Further, the energy consumption decreases because the energy deposition directed toward oxygen excitation increases, as was already explained in the gap distance results.

Previous work has shown that, for a change from a pure-methane feed to a 3:1 methane/oxygen feed, the methane reaction rate is enhanced because of the active oxygen species. In addition, organic oxygenate products are formed only when oxygen is present.[5] This work varies the methane/oxygen feed ratio from 5:1 to 2:1 at 1 and 2 atm. This is done to determine the effect of the partial pressure of oxygen on the methane reaction rate, the system's energy consumption per molecule of methane converted, and the product selectivities. Table 5 shows that, at both 1 and 2 atm, increasing the oxygen partial pressure decreases the systems' energy consumption per molecule of methane converted for a change from a 5:1 to 2:1 methane/oxygen system. This is because the methane conversion increases enough to more than compensate for the 20% decrease in methane partial pressure and throughput in both cases. The methane reaction rate, therefore, increases with increasing partial pressure of *oxygen* in the feed, which causes the decrease in energy consumption per molecule of methane converted.

Table 5. CH_4/O_2 Ratio Experimental Results[a]

CH_4/O_2	*P* (atm)	*E*/*P* [V/(cm Torr)]	conversion		eV per molecule of CH_4 converted	mol of CH_4 converted (mol/min)
			CH_4	O_2		
5:1	1	30	6	31	61	0.0012
4:1	1	30	6	27	60	0.0012
3:1	1	30	7	23	58	0.0013
2:1	1	30	9	22	48	0.0015
5:1	2	23	5	21	39	0.0019
4:1	2	23	6	19	32	0.0023
3:1	2	23	7	19	27	0.0027
2:1	2	23	8	17	26	0.0028

[a] 4.0-mm gas gap, 118-W power input, water jacket temperature = 15 °C.

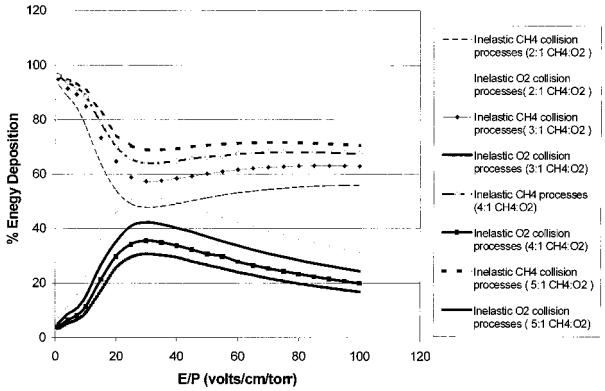

Figure 11. Energy deposition (group processes) vs *E*/*P*.

Figure 11 shows the energy deposition directed toward methane and oxygen inelastic collision processes as functions of the reduced electric field for the 5:1 and 2:1 experiments. The figure shows that, as the methane/oxygen ratio decreases, the energy deposition directed toward inelastic methane collision processes decreases, and the energy deposition directed toward inelastic oxygen collision processes increases. This is because the probability of methane colliding with an electron decreases and that of oxygen colliding with an electron increases when the methane/oxygen ratio decreases. However, the trends seen in the inelastic methane and oxygen collision process curves are similar to the trends seen in all other inelastic collision process curves for the same group. Figures 12−14 show the 5:1 to 2:1 methane/oxygen systems' energy deposition directed toward methane excitation, oxygen excitation, and oxygen dissociation, respectively. Here again, as the methane/oxygen ratio decreases, the energy deposition directed toward methane excitation decreases, while the energy directed toward oxygen excitation and dissociation increases because of the decreased probability of electrons impacting methane molecules rather than oxygen molecules. However, the trend in each curve

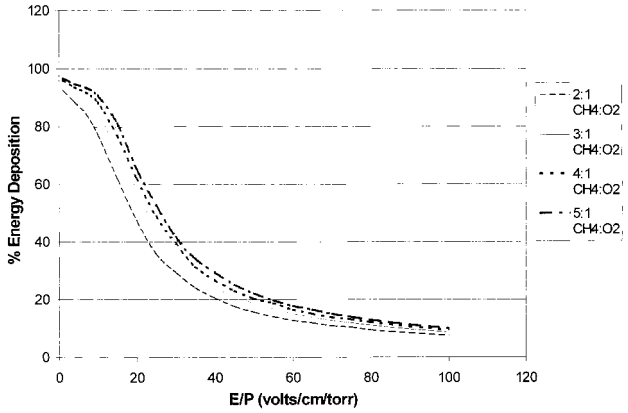

Figure 12. CH_4 excitation energy deposition vs *E*/*P*.

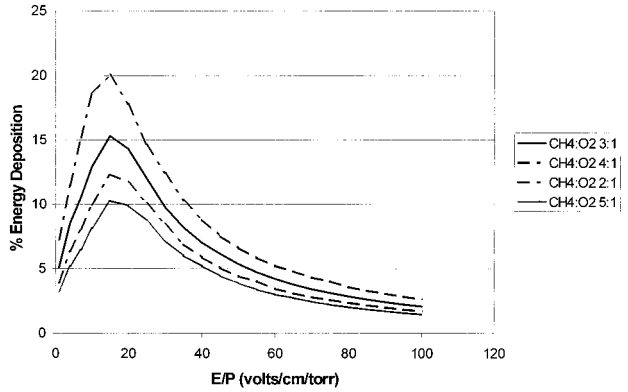

Figure 13. O_2 excitation energy deposition vs *E*/*P*.

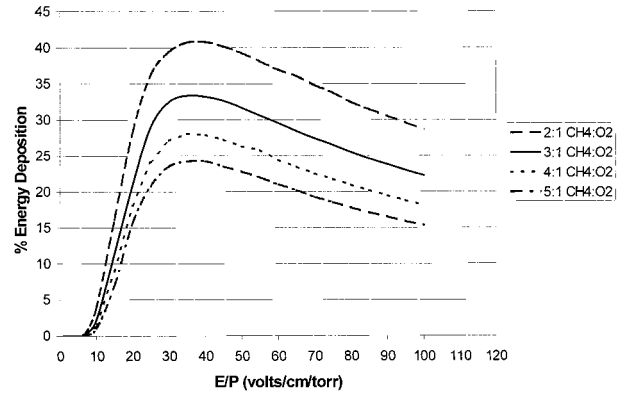

Figure 14. O_2 dissociation energy deposition vs *E*/*P*.

within a group (methane excitation group, oxygen excitation group, and oxygen dissociation group) is similar to the trend of all other curves within that group. Hence, regardless of the methane/oxygen ratio, the trends of the changes in energy deposition directed toward these collision processes due to changes of the reduced electric field are the same.

Table 6 shows the product selectivity results for the methane/oxygen feed-ratio experiments at 1 and 2 atm. At a system pressure of 1 atm, the results show that, for a change from a 5:1 to 2:1 methane/oxygen feed ratio, the CO_x, C_2, and organic oxygenate selectivities remain relatively constant. Previous work, as well as the residence-time experiments discussed later in this work, provides evidence that there is a pathway for partial oxidation of methane directly to CO and CO_2 in the dielectric barrier discharge methane/oxygen system.[11] With this in mind, the CO_x and organic oxygenate selectivities remain relatively constant when the partial pressure of oxygen is increased in the feed because both pathways are enhanced. The net effect is that changes in the rates of these two oxidative pathways balance one another. In addition, the ethane selectivity always remains low because enough atomic oxygen is present at this reduced electric field strength to consume activated methane, which limits methane coupling.

At a system pressure of 2 atm, Table 6 shows that, for a change from a 5:1 to a 2:1 methane/oxygen system, the C_2 selectivity decreases, and the organic oxygenate selectivity increases. At this reduced electric field, the energy deposition directed toward oxygen dissociation becomes sufficiently limited that increasing the partial pressure of oxygen in the feed increases the energy deposition directed toward oxygen dissociation enough to result in shifting the selectivity from C_2 species to organic oxygenate products. Finally, the CO_x selectivity in this range remains relatively constant because both the direct and the indirect methane oxidation routes to CO_x, as well as the methane oxidation routes to organic oxygenates, are being enhanced.

Increasing the system's pressure increases the feed concentration and, therefore, contributes (assuming positive-order kinetics) to the enhancement of the methane reaction rate, resulting in a decrease in the energy consumption per molecule of methane converted, as was shown in Table 5. However, as shown in Table 6, the increase in pressure also results in a decrease in the organic oxygenate selectivities because energy deposition directed toward oxygen dissociation decreases significantly.

The next series of experiments increased the system pressure from 1 to 2 atm in a 5:1 methane/system with a 1.9-mm gas gap, to compare the other results to those of the 4.0-mm gas gap. In addition, a 3-atm experiment with a 1.9-mm gas gap (5:1 methane/oxygen system)

Table 6. CH_4/O_2 Ratio Experimental Results[a]

		% selectivity[b]												
CH_4/O_2	*P* (atm)	H_2	CO	CO_2	ethane	ethylene	acetylene	M	F	MF	FA	C_2 sum	organic oxygenate liquid sum	sum
5:1	1	12	16	10	4	0	0	19	12	8	13	4	51	81
4:1	1	11	16	10	4	0	0	19	15	10	15	4	59	89
3:1	1	9	15	10	2	0	0	16	15	7	16	2	53	80
2:1	1	8	16	13	1	0	0	15	14	10	20	1	59	89
5:1	2	48	26	8	14	5	14	5	7	2	11	33	24	91
4:1	2	42	25	7	11	3	11	5	8	2	12	25	27	84
3:1	2	39	27	7	9	2	10	5	8	2	13	21	29	84
2:1	2	39	33	8	7	1	9	7	10	3	17	17	37	95

[a] 4.0-mm gas gap, 118-W power input, water jacket temperature = 15 °C, *E*/*P* = 30 V/(cm Torr) at 1 atm, *E*/*P* = 23 V/(cm Torr) at 2 atm. [b] M = methanol, F = formaldehyde, MF = methyl formate, FA = formic acid, sum = sum of carbon selectivities (molar basis). Selectivity for carbon compounds is on a carbon molar basis.

Table 7. Pressure Experimental Results[a,b]

reactor pressure (atm)	gap distance (mm)	*E*/*P* [V/(cm Torr)]	eV per molecule of CH_4 converted	mol of CH_4 converted (mol/min)	% conversion		% selectivity[c]					
					CH_4	O_2	H_2	CO	CO_2	C_2 sum	organic oxygenate liquid sum	sum
1	1.9	49	79	0.0009	10	61	18	16	13	5	51	85
2	1.9	37	51	0.0014	8	37	32	19	7	29	46	101
3	1.9	32	43	0.0017	6	24	40	22	6	30	42	100
1	4.0	30	61	0.0012	6	31	12	16	10	4	51	81
2	4.0	23	39	0.0019	5	21	48	26	8	33	24	91

[a] 1.9- and 4.0-mm gap distances. [b] 5:1 CH_4/O_2 ratio, 118-W Power Input, 15 °C water jacket temperature. [c] Selectivity for carbon compounds is on a carbon molar basis, sum = sum of carbon selectivities (molar basis).

was also performed. Table 7 shows that, for a change from 1 to 2 atm, the 1.9- and 4.0-mm-gap-distance systems exhibit 25 and 22% decreases in methane conversion, respectively. The energy consumption per molecule converted decreases 35% for the 1.9-mm-gap-distance experiment and 36% for the 4.0-mm-gap-distance system because the methane throughput doubles for both systems. This means that the methane reaction rate increases for both gap distances. Assuming positive-order kinetics, this increase could be expected because the feed concentration is doubled in both cases. In addition, for the 4.0-mm-gap-distance experiment, the energy consumption per molecule of methane converted also decreases, which can be attributed to an increase in the energy deposition directed toward methane and oxygen excitations and a decrease in the energy deposition directed toward oxygen dissociation. The 4.0-mm-gap system's energy consumption per molecule of methane converted is 22% less at 1 atm and 23% less at 2 atm than the corresponding 1.9-mm-gap system's energy consumption per molecule of methane converted. The difference seen in energy consumption per converted methane at 1 atm arises because of the decrease in the reaction volume to electrode surface area ratio (which increases radical quenching) for a change from the 4.0- to the 1.9-mm gap distance.

At 2 atm, the increase in energy consumption per molecule of methane converted for a change from the 4.0- to the 1.9-mm gap distance is because of radical quenching (the reaction volume to electrode surface area ratio decreases). Once again, the energy consumption per molecule of methane converted also increases when the gap distance is decreased because of the shift in the energy deposition from excitations of methane and oxygen to oxygen dissociation. Finally, an increase from 2 to 3 atm with the 1.9-mm gas gap resulted in a 20% decrease in the methane conversion. However, the energy consumption per molecule of methane converted decreased by 17% because the methane throughput increased by 33%. More specifically, the energy consumption per molecule of methane converted decreased as a result of an increase in the methane reaction rate because of the increase in the feed concentration.

Table 7 shows that an increase from 1 to 2 atm in the 1.9-mm-gas-gap system shifts the selectivity from organic oxygenate products to C_2 species. Again, the increase in pressure promotes methane coupling. In this same range, however, the CO selectivity increases, and the CO_2 selectivity decreases, despite the fact that the energy deposition directed toward oxygen dissociation remains significant. This suggests that oxidation of C_2 species to CO is favored over complete overoxidation to CO_2. In addition, shifts in selectivity from CO to CO_2 via the water−gas shift reaction are not seen because the selectivity to hydrogen is high and, therefore, the

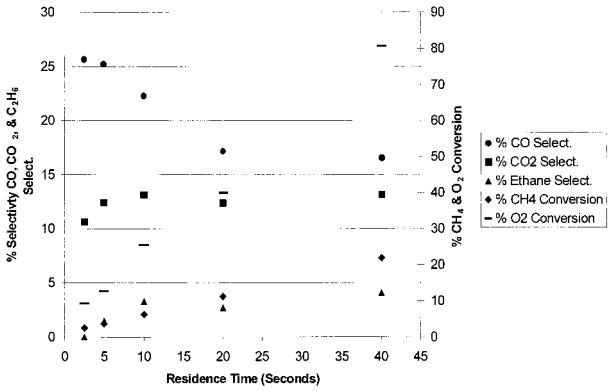

Figure 15. CH_4 and O_2 conversions and CO, CO_2, and C_2H_6 selectivities vs residence time.

reverse water−gas shift reaction prevents an overall shift back to CO_2, as previously explained. Table 6 also shows that the product selectivities at 1 atm for the 1.9- and 4.0-mm-gap-distance systems are similar. This is because the energy depositions into inelastic methane and oxygen collisions processes are similar. However, for a change from 1 to 2 atm, a greater shift in selectivity from organic oxygenate products to C_2 species occurs in the 4.0-mm-gas-gap system because of both the increase in pressure and the change in energy deposition. Thus, under all of the system variables tested, higher energy deposition directed toward oxygen dissociation enhances the organic oxygenate production.

The last experimental series studied the organic oxygenate pathways that occur once atomic oxygen initiates the process. This was done by varying the residence time for a 3:1 methane/oxygen system at 1 atm. In addition, the effects of residence time on CO_x and ethane selectivity, as well as methane and oxygen conversion were examined. Figure 15 shows the results of the latter. As the residence time is increased from 2.5 to 40 s, both the methane and oxygen conversions increase by 89%. The increases for both conversions were linear over this range, but previous work has shown that, at greater methane and oxygen conversions, the methane and oxygen conversions become nonlinear, and therefore, the methane and oxygen concentrations do affect the methane reaction rate.[11]

Figure 15 also shows the effects of residence time on the CO, CO_2, and ethane selectivities. As can be seen in the figure, the CO and CO_2 selectivities were always high. This suggests a direct oxidative pathway from methane to CO and/or CO_2. In addition, the CO_2 selectivity remains constant throughout the entire residence time range, but the CO selectivity decreases initially and then levels off at about a 20-s residence time, where it then remains constant at longer residence times. The initial decrease in the CO selectivity is due

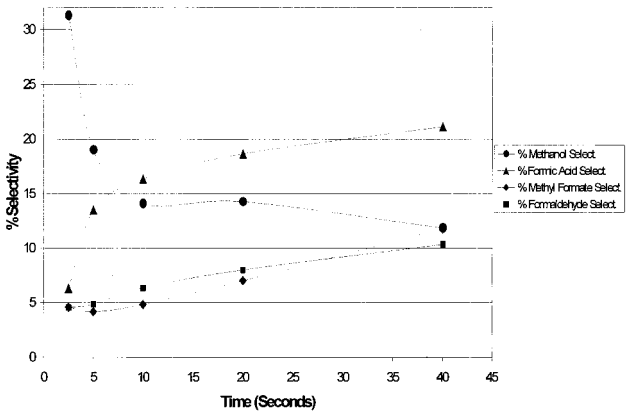

Figure 16. Organic oxygenate selectivity vs residence time.

to the water−gas shift reaction and the fact that in situ organic oxygenate product removal starts to occur as these partial pressures increase above their vapor pressures, with longer residence times resulting in condensation within the reaction zone.[10] In situ product removal also causes a decrease in the CO_2 production as less overoxidation results. The water−gas shift reaction, which increases CO_2 production, balances this change, and as shown in earlier work,[10] the CO_2 selectivity remains relatively constant.

Figure 16 shows the residence-time experiment results for the organic oxygenate selectivities (the lines included in this figure are only for illustration purposes). The figure shows that when the residence time increases from 2.5 to 40 s, the methanol selectivity initially decreases rapidly and then decreases more gradually over time. The formic acid selectivity initially increases rapidly and then at a lower rate. The formaldehyde and methyl formate selectivities increase at a uniform rate. These results indicate that methane and oxygen react to form methanol as an initial product, which further reacts to form formic acid and formaldehyde. Significant amounts of formic acid are evidently formed from methanol at relatively short residence times and can then react with methanol to form methyl formate. Finally, the organic oxygenate selectivities at the 40-s residence time represent the typical selectivities seen with longer-residence-time experiments (residence time $\geq$ 40 s).

Conclusions

The product selectivities in a methane/oxygen system within a DBD reactor can be affected by altering the reduced electric field strength by changing the geometry or operating conditions. These changes affect the average electron energy within the system and can shift the energy deposition among the various collision processes. This was shown in a 2:1 methane/oxygen system through the shift in product selectivities from organic oxygenate products to C_2 species when the reduced electric field strength is changed from 30 to 18 V/(cm Torr) by increasing the gap distance from 4.0 to 12.0 mm.

The results for a 2:1 methane/oxygen system with a 4.0-mm gap distance at elevated pressure verified that the shift in product selectivities from organic oxygenates to C_2 species could be attributed to the decrease in the reduced electric field. The effect of pressure on the results showed a similar shift in product selectivities when the reduced electric field was changed over the same range as in the gap-distance experiments. However, it was found that increasing the system pressure also promotes methane coupling.

The energy consumption per molecule of methane converted was affected by the methane/oxygen feed ratio, the system pressure, the reduced electric field strength, and the reaction volume to electrode surface area ratio. Higher partial pressures of oxygen in the feed were found to decrease the energy consumption per molecule of methane converted, which is consistent with prior work.[4] Increasing the pressure also reduces the system's energy consumption per molecule of methane converted because of the increases in the feed concentration. However, significant reductions in the organic oxygenate selectivity occur if the reduced electric field strength is too low. Large decreases in the system's energy consumption per molecule of methane converted (as high as 55%), which are solely due to decreases in the reduced electric field strength (at constant feed concentration), come with significant losses (as high as 65%) in the organic oxygenate product selectivity.

The increase in the CO/CO_2 ratio when the pressure is increased from 1 to 2 atm, or the gap distance is increased from 4.0 to 12.0 mm, might be a result of partial oxidation of C_2 species to CO being favored over complete overoxidation to CO_2. In addition, if the reduced electric field is low enough that a decrease in energy deposition directed toward atomic oxygen occurs, the CO/CO_2 ratio can be expected to increase.

Residence time studies showed that methane partially oxidizes to form methanol, which further reacts to form formic acid, formaldehyde, and methyl formate. This experimental series supports the conclusion that there is a direct oxidative route from methane to CO and/or CO_2 as significant amounts of both are present at even low residence times, which is consistent with previous work.[11] All of the results are consistent with the changes of the populations of active species with changes in energy deposition due to changes in the reduced electric field. In the range studied, a lower reduced electric field reduces oxygen dissociation and increases methane and oxygen excitations. Lower oxygen dissociation reduces organic oxygenates, but higher methane and oxygen excitations decrease energy consumption per molecule of methane converted.

Finally, with regard to energy usage, the best results in this study are 26 eV per molecule of methane converted. Because all products except for CO_2 might be considered useful, the system requires 28 eV per molecule of useable carbon produced. A large-scale commercial methanol synthesis process consumes 11 eV per molecule of methanol produced.[18] However, at a remote site the one-step partial oxidation of methane to organic oxygenates using a DBD reactor might be feasible despite the higher energy consumptions because of the increased simplicity and lower capital costs compared to conventional processes. Therefore, further reductions in power consumption remain desirable, but the exact level that is required will depend on the specifics of a given gas-conversion project.

Acknowledgment

The support of Texaco, Inc.; the National Science Foundation for a Graduate Traineeship; and the United States Department of Energy under Contract DE-FG21-94MC31170 are gratefully acknowledged.

Literature Cited

(1) Chang, J. S.; Lawless, P. A.; Yamamoto, T. Corona Discharge Processes. *IEEE Trans. Plasma Sci.* **1991**, *19* (6), 1152−1166.

(2) Eliasson, B.; Kogelschatz, U. Nonequilibrium Volume Plasma Chemical Processing. *IEEE Trans. Plasma Sci.* **1991**, *19* (6), 1063−1077.

(3) Bruno, G.; Capezzuto, P.; Cicala, G. *Chemistry of Amorphous Silicon Deposition Processes: Fundamentals and Controversial Aspects*; Academic Press: New York, 1995.

(4) Bhatnagar, R.; Mallinson, R. G. Methane Conversion in AC Electric Discharges at Ambient Conditions. In *Methane and Alkane Conversion Chemistry*; Plenum Press: New York, 1995; pp 249−264.

(5) Larkin, D. W.; Caldwell, T. A.; Lobban, L. L.; Mallinson, R. G. Oxygen Pathways and Carbon Dioxide Utilization in Methane Partial Oxidation in Ambient Temperature Electric Discharges. *Energy Fuels* **1998**, *12* (4), 740−744.

(6) Zhou, L. M.; Xue, B.; Kogelschatz; U.; Eliasson, B. Partial Oxidation of Methane to Methanol with Oxygen or Air in a Nonequilibrium Discharge Plasma. *Plasma Chem. Plasma Process.* **1998**, *18* (3), 375−393.

(7) Pitchford, L. C.; Boeuf, J. P.; Morgan, W. L. *Bolsig*; Collaboration between CPAT, Toulouse, France, and Kinema Software, Monument, CO, 1995. This freeware is available at http://cpat.ups-tlse.fr/operations/operation_03/POSTERS/BOLSIG/..

(8) Pitchford, L. C.; Oneil, S. V.; Rumble, J. R. Extended Boltzmann Analysis of Electron Swarm Parameters. *Phys. Rev. A* **1980**, *23* (1), 294−304.

(9) Zhou, L.-M. *Non-Thermal Plasma Features in Dielectric Barrier Discharges*; Institute for Gas Utilization Technologies, University of Oklahoma: Norman, OK, 1998.

(10) Larkin, D. W.; Leethochawalit, S.; Caldwell, T. A.; Lobban, L. L.; Mallinson, R. G. Carbon Pathways, CO_2 Utilizaton, and In Situ Product Removal in Low-Temperature Plasma Methane Conversion to Methanol. In *Greenhouse Gas Control Technologies*; Elsevier Science Ltd.: New York, 1999; pp 397−402.

(11) Larkin, D. W.; Lobban, L. L.; Mallinson, R. G. Production of Organic Oxygenates in the Partial Oxidation of Methane in a Silent Electric Discharge Reactor. *Ind. Eng. Chem. Res.* **2001**, *40* (7), 1594−1601.

(12) Eliasson, B.; Elgi, W.; Kogelschatz, U. Modeling of Dielectric Barrier Discharge Chemistry. *Pure Appl. Chem.* **1994**, *66* (6), 1275−1286.

(13) *The Siglo Data Base*; Collaboration between CPAT, Toulouse, France, and Kinema Software, Monument, CO, 1995. For additional information, see http://www.siglo-kinema.com.

(14) Mizuno, A.; Katsura, S.; Okumoto, M. *Direct Synthesis of Methanol using Non-Thermal Plasma*; Research Project Report No. 256; Ministry of Education of Japan: Tokyo, Japan, 1998; pp 21−27.

(15) Caldwell, T. A. The University of Oklahoma, Norman, OK, 2001, personal communication.

(16) Tas, M. A. Plasma-Induced Catalysis: A Feasibility Study and Fundamentals. Ph.D. Thesis, Eindhoven University of Technology, Eidhoven, The Netherlands, 1995.

(17) Khan, A. A. Studies on the Inhomogeneous Nature of the Silent Discharge Reactor: Part 1. Experimental Investigations. *Can. J. Chem. Eng.* **1989**, *67*, 102−106.

(18) Rostrup-Nielson, J. R. Catalysis and Large-Scale Conversion of Natural Gas. *Catal. Today* **1994**, *21*, 257−267.

Received for review April 2, 2001
Revised manuscript received August 16, 2001
Accepted August 27, 2001

IE010298H